Progress In Electromagnetics Research C, Vol. 76, 109–118, 2017

Very Compact 5.5 GHz Band-Notched UWB-MIMO Antennas with High Isolation

Zhiwei Liu*, Xiliang Wu, Yueyuan Zhang, Peng Ye, Zhiqing Ding, and Cheng Hu

Abstract—Two different types of band-notch UWB-MIMO antennas are proposed in this paper. The filtering effect can be achieved by integrating slot resonators to a UWB antenna. Both of the proposed antennas have very compact size and are smaller than most of the other band-notch UWB-MIMO antennas. The ultra-wideband is achieved by etching stepped slots on the ground. The band-notch characteristic can greatly reduce the potential interference between the UWB and WIMAX/WLAN system. Our proposed antennas can also possess a wide bandwidth from 3 GHz to 11 GHz with $|S_{11}| < -10\,\text{dB}$. Some effective measures have been taken and illustrated to reduce the isolation. Measurements demonstrate that the mutual coupling between the antenna elements is good enough for a MIMO system. Their stable radiation patterns are simulated, designed and measured successfully. The good performance and compact size make the antennas good candidates for UWB applications.

1. INTRODUCTION

Ultra-wideband (UWB) wireless communication has attractive application prospects. Compared with traditional narrow-band and wide-band wireless communication systems such as Blue-tooth technology, UWB technology can provide much higher transmission rate. Besides, a UWB system offers some other unique and distinctive properties, for instance, lower emission power, lower cost and more security [1], which make it more attractive than other short-range wireless communication technologies. In wireless local area networks and home audio/visual network applications such as high-speed high-definition television (HDTV) and audio/visual streams [2], people pay more attention to high-data-rate, near 1 GB/s transmission rate. In order to achieve the requirement, more advanced techniques are needed. UWB combined with multi-input multi-output (MIMO) technology should be a wonderful solution. Some MIMO antennas for UWB applications have been proposed in the past few years [3–6].

The Federal Communication Commission (FCC) released the frequency band from 3.1 GHz to 10.6 GHz for commercial communication applications in 2002 [7]. Over the entire UWB, some other narrow-band systems already exist [8, 9], such as wireless local area network (WLAN) operating in 5.15–5.85 GHz and WIMAX in the 3.3–3.7 GHz. These existing narrow-band communication systems will inevitably interfere with the UWB system. In order to minimize the interference between the narrow-band system and UWB system, the UWB antennas with band-notch characteristics have been introduced. Many band-notch antennas are achieved by cutting slots in the radiator [10, 11], and some other UWB band-rejection antennas are also implemented by etching slots on the ground [12]. Moreover, controlling the resonant frequency of the antenna is an an efficient way to achieve band-rejection feature [13].

Body area network systems are useful and have great potential for several applications. The advantage of low emission power and high data rate will make UWB technology a promising candidate for body area networks. Two similar UWB-MIMO antennas with WLAN band rejection are proposed,

Received 30 May 2017, Accepted 12 July 2017, Scheduled 31 July 2017
* Corresponding author: Zhiwei Liu (zwliu1982@hotmail.com).
The authors are with the East China Jiaotong University, Nanchang 330013, China.

which is used for a sensor device of body area network. Etching two symmetrical half-wavelength or quarter-wavelength slots on the ground, a notch band at 5.5 GHz is achieved. The frequency can be adjusted easily by changing the length and width of these slots. A T-shape slot and rectangular slots cut down on the ground are to reduce the coupling between the two radiator elements as well as enhance the isolation. The ANSOFT simulation software high-frequency structure simulator (HFSS) based on the finite element method (FEM) is used for designing, optimizing and simulating the proposed antennas.

2. UWB-MIMO ANTENNAS DESIGN

Recently, some antennas with UWB characteristic have been proposed. Among these design methods, one of them is to apply a stepped structure, such as gradient or cambered shapes to obtain the UWB antenna [14]. These UWB-MIMO antennas with stepped slots on the ground have already been presented [15–18]. However, there is interference between the UWB and conventional narrow-band systems. Therefore, it is extremely necessary to design a UWB-MIMO antenna with the feature of band-notch. Fig. 1 shows two types of UWB-MIMO antennas with 5.5 GHz rejection. Both, printed on the FR4 substrate, have compact size of 22 mm × 29 mm, thickness of 0.8 mm and relative dielectric constant of 4.4. The top layer consists of two 50 Ω microstrip lines (microstrips with 50 Ω), and the bottom is a metal ground with several slots. Both slots in *Antenna*-1 and *Antenna*-2 (the two antennas are same except the metal ground plane) are designed to achieve 5.5 GHz band-notch, while the shapes of the two slots are different. Each slot acts as one resonator. The resonant frequency of slots mainly depends on the length of the slots. The wavelength can be calculated using the following formula:

$$\lambda = \frac{c}{f \cdot \sqrt{\varepsilon_{eff}}} \tag{1}$$

where c is the speed of the light, f the designed band-notch frequency, and ε_{eff} the effective dielectric constant. As shown in Fig. 1, *Antenna*-1 applies two symmetrical C-shape slots which are about half-wavelength of the notch-band frequency etched in the middle of the ground. The length of the C-shape slot can be deduced by

$$L_{slot\text{-}c} = c_1 + c_2 + c_3 \approx \frac{\lambda}{2} \tag{2}$$

However, different locations has different slot lengths. In Fig. 2, slots are located on the edge of ground, and one end of each slot is open. The length is only about a quarter wavelength. In *Antenna*-2, two Z-shape slots with near quarter-wavelength are introduced. The length of the Z-shape can be calculated by

$$L_{slot\text{-}z} = z_1 + z_2 + z_3 \approx \frac{\lambda}{4} \tag{3}$$

The EM software ANSOFT HFSS is used to design and optimize antennas. The final parameters are shown in Table 1.

Table 1. Parameters of the proposed antennas. (Unit: mm).

L_1	W_1	U_1	U_2	T_1	F_1	D_1	D_2	C_1	C_2	C_3	Z_1	Z_2	Z_3	F_2
22	30	5	3.5	7.5	15	15.1	7.5	2.6	4	7.5	2.5	3.1	3.5	2

Both quarter-wavelength slots and half-wavelength slots make the impedance at the band of 5–6 GHz worse and have little influence on the isolation between antenna elements, which is proved by the comparison of results shown in Fig. 4. Electric field distributions at 5.5 GHz for the MIMO antenna without slot, with half wavelength slot and with quarter wavelength slot are displayed in Fig. 2. It is obvious that the slots change the antenna's electric field distribution. The electric field of the antenna with slots is mainly concentrated on the slots. This leads to the impedance mismatch. Fig. 3 Shows the impedance of the MIMO antenna against the frequency. In this figure, it is clearly shown that the impedance values of the antenna with slot change greatly at the band of 5–6 GHz, especially the antenna with $\lambda/2$ slot. Comparing (b) with (c), both the slots achieve band-notch characteristic; however, the

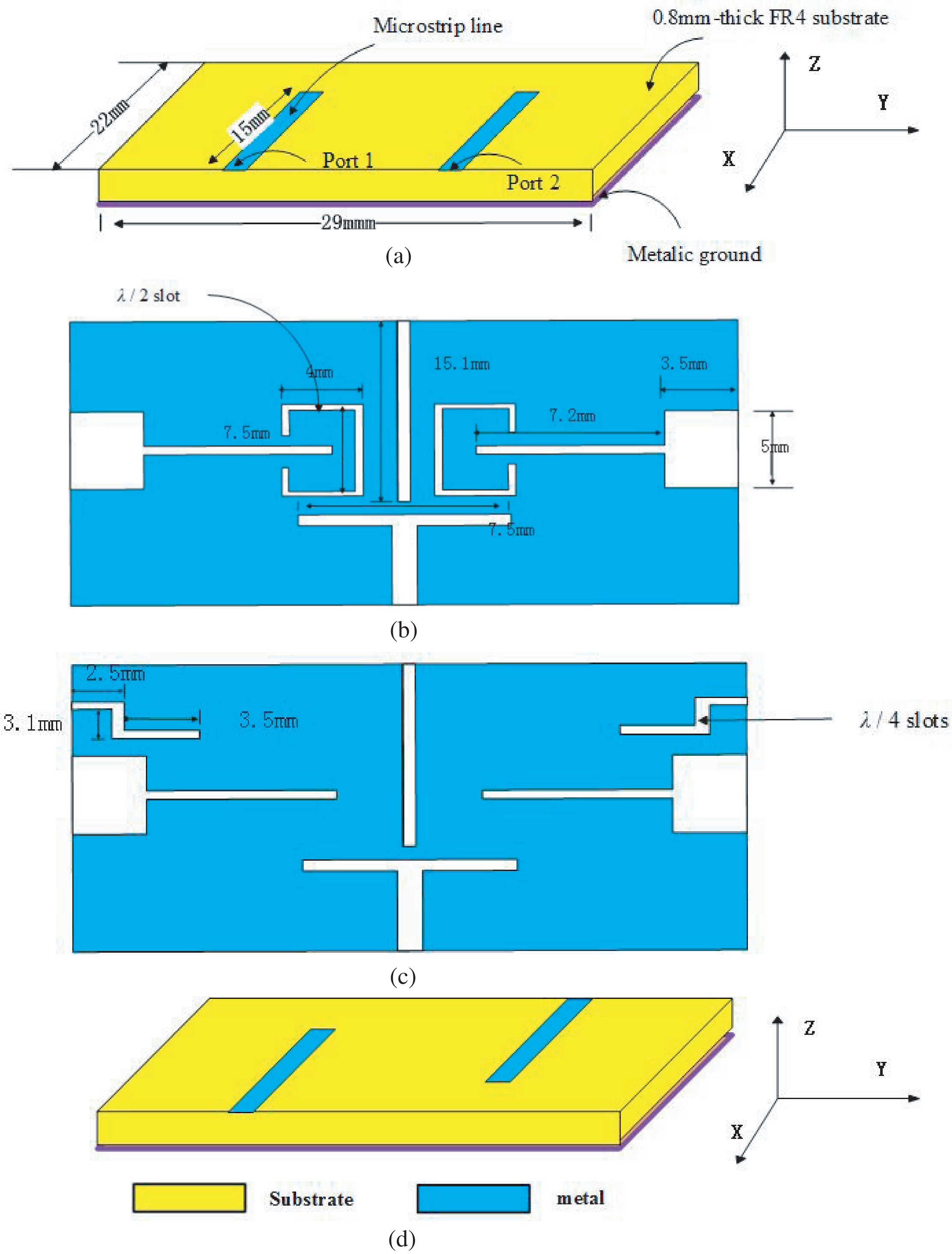

Figure 1. Structure of the proposed band-rejection UWB-MIMO antennas: (a) the overall diagram of the antenna, (b) metallic ground with $\lambda/2$ slots (*Antenna*-1), (c) metallic ground with $\lambda/4$ slots (*Antenna*-2), (d) the improvement of antenna 2 (*Antenna*-3).

antenna with $\lambda/4$ slot is better than that antenna with $\lambda/2$ slot. For MIMO antennas, isolation among the elements is an important property. It reflects the degree of mutual coupling between the antenna elements. The isolation of antenna 1 is a little worse. In order to improve the isolation, a T-shaped slot

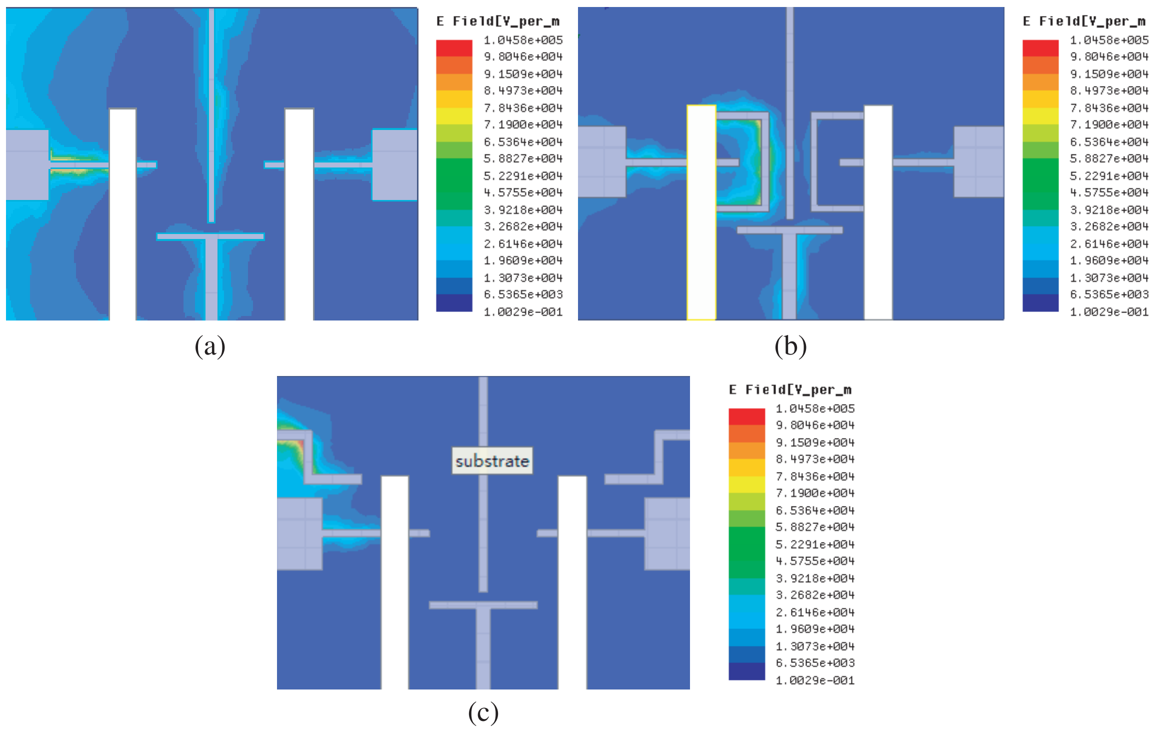

(c)

Figure 2. Electric field distribution on MIMO antenna: (a) without slot, (b) with $\lambda/2$ slot, (c) with $\lambda/4$ slot.

and two rectangular slots are cut down on the ground. To further reduce the mutual coupling, one port can be placed on the other side of the substrate. Fig. 1(d) reveals the improved MIMO antenna named as "*Antenna*-3".

Table 2 compares the proposed antenna with the most representative UWB-MIMO antennas presented in the literature. The list is not comprehensive but fairly represents the current state of the art of this technology. Though the antenna size in [6] is smaller than the proposed antenna, the proposed antenna can achieve WLAN band rejection, and the antenna in [6] cannot. Besides, the ECC of the proposed antenna is better, and the isolation is also good enough.

Table 2. Performance comparison with previous published literature.

Publication literature	PCB size	Band-width (GHz)	Isolation (dB)	Gain var-(dBi)/ total efficiency, %	ECC using far-field patterns
[3] Khan	33×45.5	3.1–10.6	< -15	2.3/85	< 0.6
[4] J. Ren	32×32	3.1–10.6	< -15	2.5/60	N.A
[5] Khan	23×39.8	3.1–10.6	< -21	2.8/82	< 0.6
[6] Khan	22×24.3	3–10.6	< -15	4/82	< 0.42
Proposed antenna	22×29	3.1–11	< -20	2.8/83	< 0.265

3. RESULTS AND DISCUSSION

In order to study the actual performance of the proposed UWB-MIMO band-notch antennas, the Agilent E5071C vector network analyzer (VNA) is used to measure the S-parameters. Fig. 5 shows the fabricated

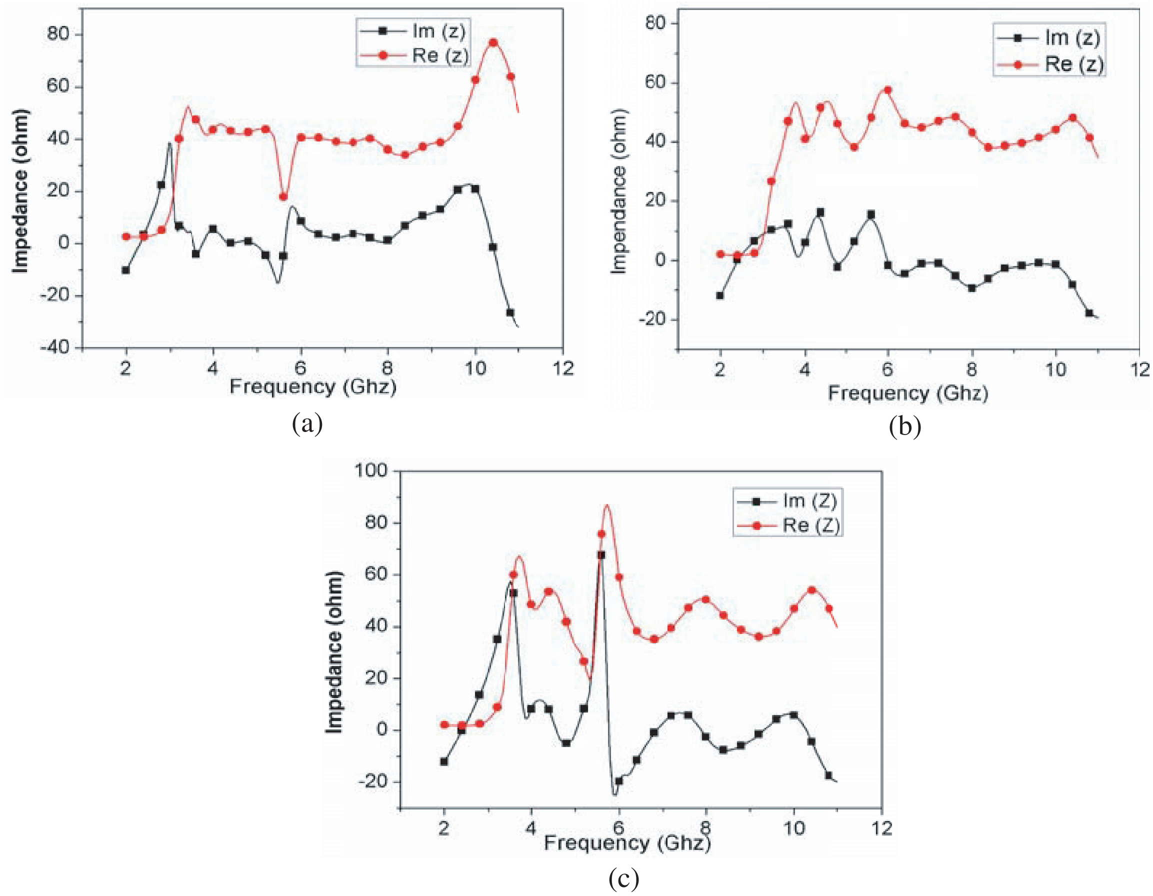

Figure 3. Impedance of the MIMO antenna over frequency: (a) without slot, (b) with $\lambda/2$ slot, (c) with $\lambda/4$ slot.

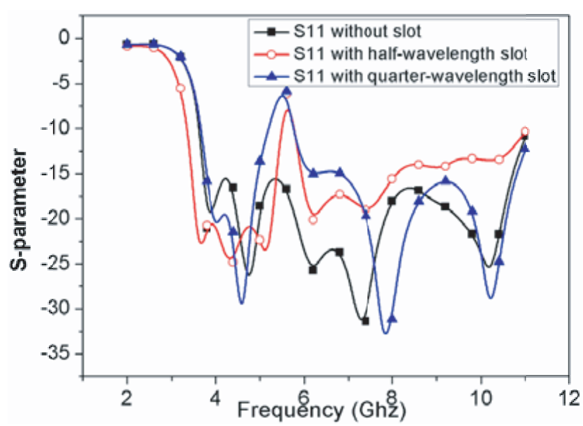

Figure 4. S_{11} curve of MIMO antenna.

prototype of the proposed antennas. To reduce interference among antenna elements and ensure the accuracy of the measurement results, a $50\,\Omega$ load is loaded into the port which is not excited. Fig. 6 show the S-parameters (S_{11}, S_{21}) of the presented *Antennas* 1, 2 and 3, respectively. These antennas have wide impedance bandwidth. The mutual coupling of *Antennas* 2 and 3 are both less than $-15\,\mathrm{dB}$ over the whole UWB (3.1–10.6 GHz). *Antenna*-2 has the best isolation ($S_{21} < -20\,\mathrm{dB}$) among the three types of antennas.

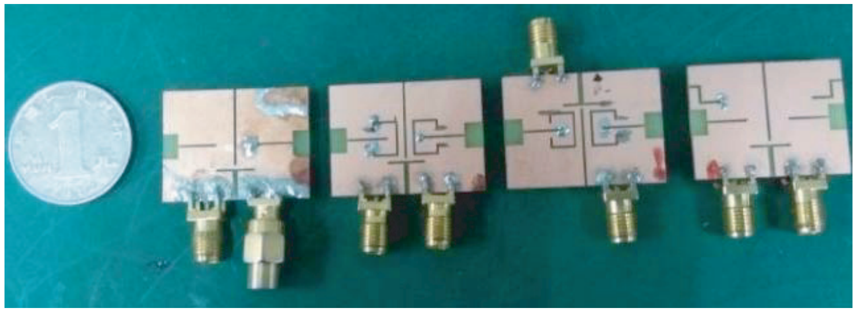

Figure 5. Prototype of the proposed antennas.

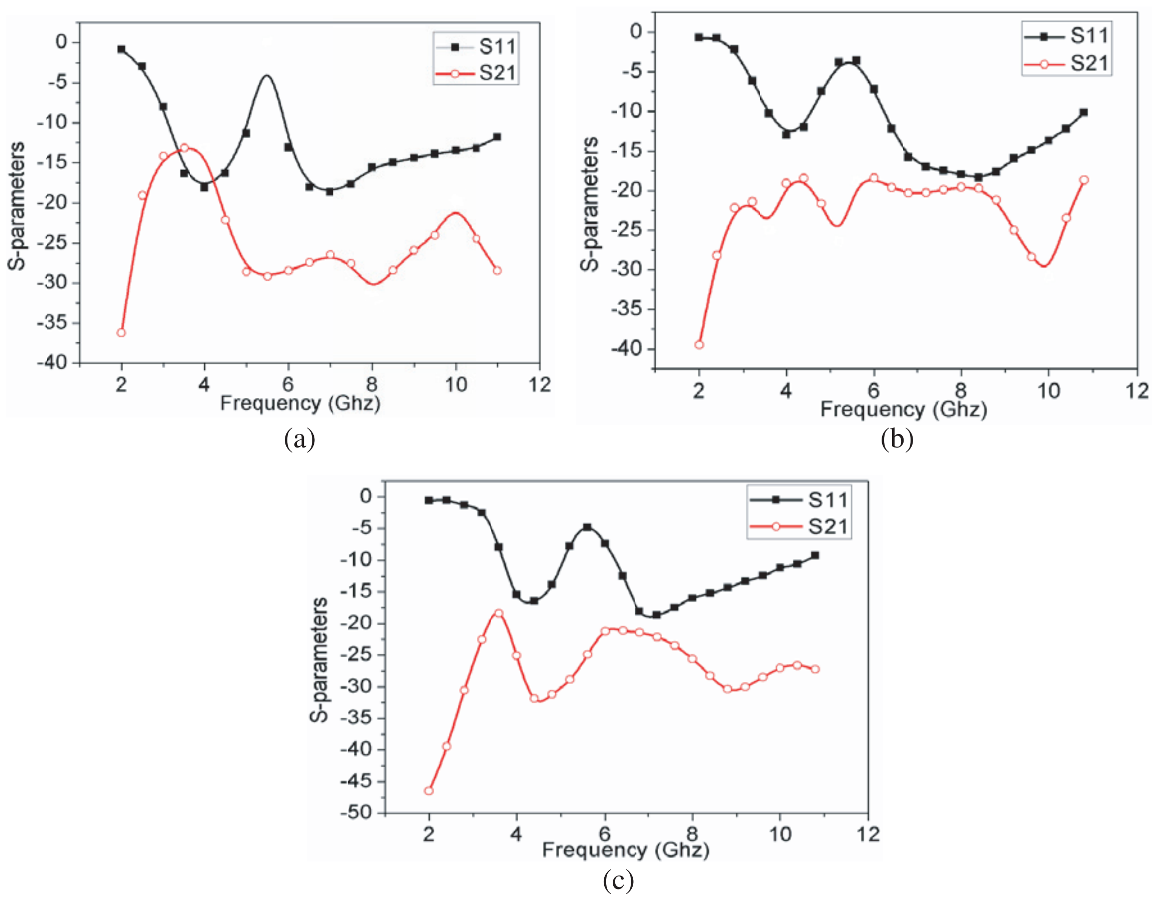

Figure 6. Measurement of S-parameters: (a) *Antenna*-1, (b) *Antenna*-2, (c) *Antenna*-3.

Envelope correlation coefficient (ECC) is an important parameter to evaluate the performance of the antenna. It is a measure that describes how much the communication channels are isolated or correlated with each other. There are two different ways to calculate the correlation factor. One is applying s-parameters to compute the correlation factor but is valid for lossless antennas only. The other method is applying the radiation pattern form, which is valid for lossy system as well. Formulations for both methods are listed as follows:

$$\rho_e = \frac{|S_{11}^* S_{12} + S_{21}^* S_{22}|^2}{(1 - |S_{11}|^2 - |S_{21}|^2)(1 - |S_{22}|^2 - |S_{12}|^2)} \tag{4}$$

$$\rho_e = \frac{\left| \iint\limits_{4\Pi} \left[F_1(\theta,\phi) \cdot F_2(\theta,\phi) \right] d\Omega \right|^2}{\iint\limits_{4\Pi} |F_1(\theta,\phi)|^2 d\Omega \iint\limits_{4\Pi} |F_2(\theta,\phi)|^2 d\Omega} \tag{5}$$

where $F_1(\theta\varphi)$ is the radiation pattern when port 1 is excited and port 2 loaded with a $50\,\Omega$ load. $F_2(\theta\varphi)$ is the radiation pattern when port 2 is excited and port 1 loaded with a $50\,\Omega$ load. Ω is the solid angle $(\theta\varphi)$. An envelope correlation coefficient value of 0.5 has been set at an acceptable value for diversity conditions. The calculation results based on the s-parameters are smaller than 0.008 within the whole operation band. Based on formula (5), $\rho_e \leq 0.265$. Although there are slight differences between these two results, both of them are smaller than 0.5. Accordingly, the correlations between elements are acceptable for the UWB MIMO system.

Figure 7 presents the measured radiation patterns (x-y, x-z, and y-z planes) at 3.5, 7, 9.5 GHz. The radiation pattern is nearly omnidirectional in the x-y plane. The peak gain and radiation efficiencies are plotted in Fig. 8. It is obvious that the antenna's peak gain and radiation efficiencies are stable at a high level; however, there is a sharp reduction in 5–6 GHz.

In practical applications, an antenna often needs to be connected to the main board. In order to study the effects of large ground, the proposed antenna 2 is connected to a large ground through a small strip in simulation as shown in Fig. 9. The simulation results of s-parameters are shown in Fig. 10. It

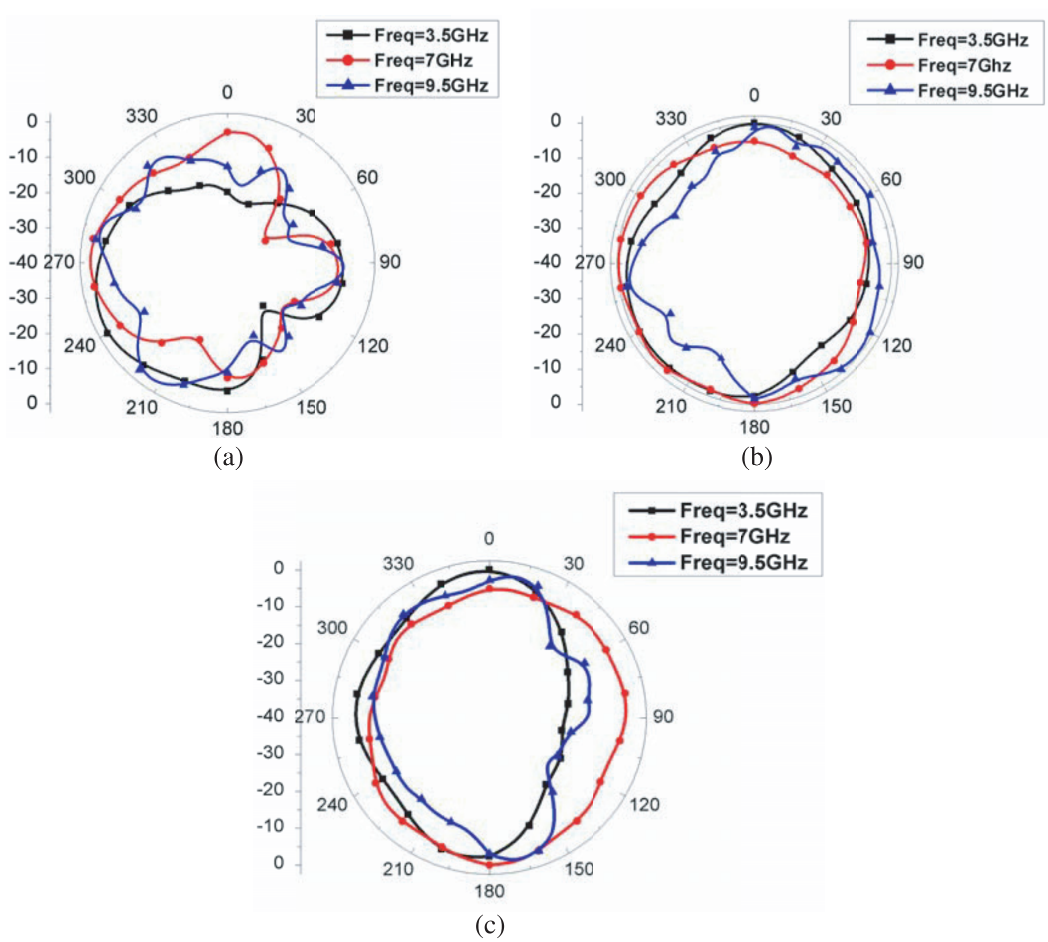

Figure 7. Measured radiation patterns of proposed *Antenna*-2 at 3.5, 7, and 9.5 GHz: (a) x-z plane, (b) x-y plane and (c) y-z plane.

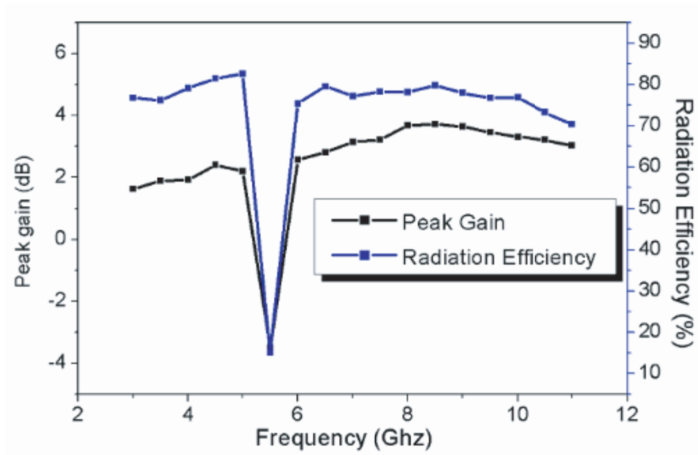

Figure 8. Measurements of gains and radiation efficiencies of *Antenna*-2.

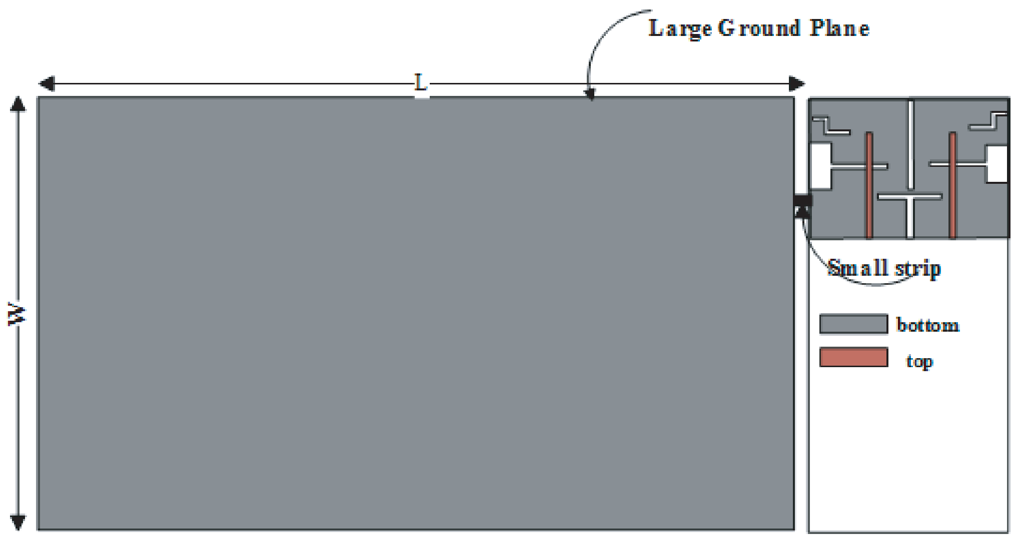

Figure 9. The proposed antenna 2 connected with a lager ground through a small strip.

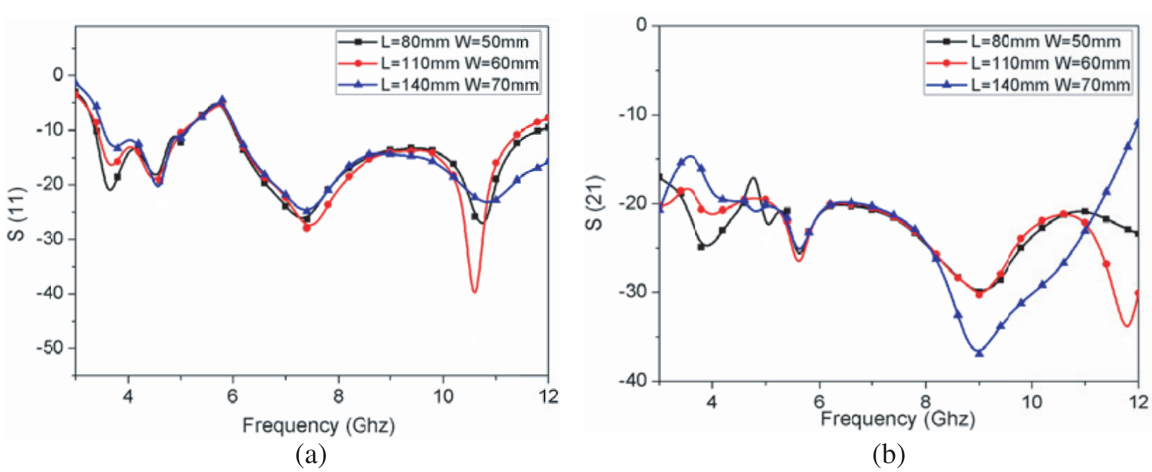

Figure 10. Effects of large ground plane on *s*-parameters: (a) S_{11}, (b) S_{21}.

is concluded that the large ground has little influence on s-parameters of the proposed antenna. The antenna performance can still meet the requirement of the UWB-MIMO system.

4. CONCLUSION

Two different types of UWB-MIMO antennas with 5.5 GHz band rejection have been proposed. By using two different types of slots, half-wavelength slot and quarter-wavelength slot, we achieve the band-notched characteristic. However, in the present design, the antenna with $\lambda/4$ antenna can achieve better band-notch feature than the antenna with $\lambda/2$. The proposed antennas have pretty good isolation ($S_{21} < -15\,\text{dB}$) and impedance ($S_{11} < -10\,\text{dB}$). It is an effective method to improve the isolation by placing two ports on different sides of the substrate. The antennas have small size and good performance, so they are suitable for wireless portable devices with UWB-MIMO antennas.

ACKNOWLEDGMENT

This work was supported by the National Natural Science Foundation of China (61601185), Natural Science Foundation of Jiangxi Province (20161BAB202062, 20171ACB21040), and Graduate Innovation Fund Project (No. YC2014-S270).

REFERENCES

1. Igor Immoreev, J., "Ultra-wideband systems. Features and ways of development," *Ultra Wideband and Ultra Short impulse signals*, 19–22, Sevastopol, Ukraine, Sept. 2004.
2. Kaiser, T., F. Zheng, and E. Dimitrov, "An overview of ultra-wide-band systems with MIMO," *Proceedings of the IEEE* Vol. 97, 285–312, Feb. 2009.
3. Khan, M. S., et al., "Compact ultra-wideband diversity antenna with a floating parasitic digitated decoupling structure," *Microw. Antenna Propag.*, Vol. 8, 747–753, Mar. 2014.
4. Ren, J., et al., "Compact printed MIMO antenna for UWB applications," *IEEE Antenna Wireless Propag. Lett.*, Vol. 13, 1517–1520, 2014.
5. Khan, M. S., et al., "Planar, compact ultra-wideband polarisation diversity antenna array," *Microw. Antennas Propag.*, Vol. 9, No. 15, 1761–17688, Dec. 2015.
6. Khan, M. S., et al., "Ultra-compact dual-polarised UWB MIMO antenna with meandered feeding lines," *Microw. Antennas Propag.*, Vol. 11, No. 7, 997–1002, 2017.
7. Federal Communications Commission (FCC), Revision of Part 15 of theCommission's Rules Regarding Ultra-Wideband Transmission Systems First Rep. and Order, ET Docket 98-153, FCC 02-48, Adopted: Feb. 2002; Released, Apr. 2002.
8. Palandöken, M., "Dual broadband antenna with compact double ring radiators for IEEE 802.11ac/b/g/n WLAN communication applications," *Turkish Journal of Electrical Engineering and Computer Sciences*, 10.3906/elk-1507-121, 2017.
9. Palandöken, M., *Artificial Materials Based Microstrip Antenna Design, Microstrip Antennas*, Prof. Nasimuddin Nasimuddin (Ed.), InTech, 2011, ISBN: 978-953-307-247-0.
10. Cho, Y. J., K. H. Kim, D. H. Choi, S. S. Lee, and S. O. Park, "A miniature UWB planar monopole antenna with 5-GHz band-rejectionfilter and the time-domain characteristics," *IEEE Trans. Antennas Propagation*, Vol. 54, 1453–1460, 2006.
11. Chu, Q. X. and Y. Y. Yang, "A compact ultrawideband antenna with 3.4/5.5 GHz dual band-notched characteristics," *IEEE Trans. Antennas Propagation*, Vol. 56, 3637–3644, Dec. 2008.
12. Gayathri, R., T. U. Jisney, D. D. Krishna, M. Gopikrishna, and C. K. Aanandan, "Band-notched inverted-cone monopole antenna for compact UWB systems," *IEE Electronics Letter*, Vol. 44, 1170–1171, Sept. 2008.
13. Schantz, H. G., "Spectral control antenna apparatus and method (Utility patent)," U.S. Patent 7 064 723 B2, Jun. 20, 2006.

14. Mehdipour, A., K. M. Aghdam, R. F. Dana, and M. R. K. Khatib, "A novel coplanar waveguide-fed slot antenna for ultrawideband applications," *IEEE Trans. Antennas Propagation*, Vol. 56, No. 12, 3857–3862, Dec. 2008.
15. Luo, C.-M., J.-S. Hong, and L.-L. Zhong, "Isolation enhancement of a very compact UWB-MIMO slot antenna with two defected ground structures," *IEEE Antennas Wireless Propagation Letters*, Vol. 14, 1766–1769, 2015.
16. Khan, M. S., A.-D. Capobianco, S. M. Asif, D. E. Anagnostou, R. M. Shubair, and B. D. Braaten, "A compact CSRR enabled UWB MIMO antenna," *IEEE Antenna and Wireless Propagation Letters*, Vol. 58, No. 6, 808–812, Aug. 2016.
17. Khan, M. S., A. D. Capobianco, A. Naqvi, M. F. Shafique, B. Ijaz, and B. D. Braaten, "Compact planar UWB MIMO antenna with on-demand WLAN rejection," *IET Electronic Letters*, Vol. 51, No. 13, 963–964, Jun. 2015.
18. Khan, M. S., A. D. Capobianco, S. Asif, A. Iftikhar, B. Ijaz, and B. D. Braaten, "Compact 4×4 UWB-MIMO antenna with WLAN band rejected operation," *IET Electronic Letters*, Vol. 51, No. 14, 1048–1050, Jul. 2015.